PHYSICAL REVIEW D

PARTICLES AND FIELDS

THIRD SERIES, VOLUME 36, NUMBER 12 15 DECEMBER 1987

Optimal design of resonant-mass gravitational wave antennas

John C. Price

Department of Physics, Stanford University, Stanford, California 94305

(Received 20 July 1987)

A new generation of resonant-mass gravitational wave antennas, to be operated at ultralow temperatures, is under development by several research groups. This paper presents a theory for the optimal design of the new antennas. First, a general sensitivity limit is derived, which may be applied to any linear instrument for which the design figure of merit is the signal-to-noise ratio (SNR). By replacing the amplifier by its noise resistance and considering the energy dissipated in the noise resistance when a signal is applied, it is possible to show that the optimally filtered SNR is less than or equal to $E_r/(kT_n)$, the energy dissipated in the noise resistance divided by Boltzmann's constant times the amplifier noise temperature. This sensitivity limit will be achieved if the instrument is lossless, in which case the energy dissipated in the noise resistance is equal to the energy deposited in the system by the signal. For resonant-mass gravitational wave antennas, if the amplifier is identified as the mechanical amplifier (transducer and electronic amplifier together), then the lossless limit is accessible in practice. A useful point of view is that optimal antenna designs are those that are most loss tolerant—those that achieve the limiting SNR with the lowest possible mechanical Q values. The techniques of network synthesis may be used to design mechanical networks for matching the main antenna mass to the mechanical amplifier that are optimal in this sense. A class of loss-tolerant networks has been synthesized; their properties are summarized in a set of design charts that give the Q requirements and bandwidth as a function of the number of modes, the temperature, and the amplifier noise resistance and noise temperature.

I. INTRODUCTION

The development of resonant-mass gravitational wave antennas has now progressed to the point where the strongest predicted events[1] are detectable. A supernova core collapse 10 kpc away (the distance to the center of the Milky Way), which converts one percent of a solar mass into radiation, will produce a pulse lasting about one millisecond with a dimensionless amplitude of $h \approx 10^{-18}$ at the Earth. This pulse gives approximately a signal-to-noise ratio (SNR) of unity for the present generation of cryogenic antennas, which are about 100 times more sensitive to gravitational wave amplitude than were the pioneering antennas constructed by Weber[2] in the 1960s. Events strong enough to detect at the present sensitivity are expected to be rare. A long-term effort, now underway, to detect multiple coincidences between widely spaced antennas offers hope for the first unambiguous detection of gravitational radiation.

Several groups are laying plans for a third generation of more sensitive resonant-mass antennas,[3] and the development of long-baseline laser interferometers as gravitational wave antennas is also being pursued.[4] For resonant-mass antennas, it is hoped that extensions of existing technology will permit pulse sensitivities of $h \approx 10^{-19}-10^{-20}$ in the next generation. Similar sensitivities may be achieved when the first generation of large (several kilometers) laser interferometers are built. Major features of the plans for resonant-mass antennas include the use of ultralow temperatures (10–50 mK), improved transducers and electronic amplifiers, improved vibration isolation, and the use of multimode mechanical impedance-matching networks.

This paper discusses the theory needed to design future generations of resonant-mass antennas. In Sec. II a sensitivity limit is derived, which extends the earlier result of Giffard[5] concerning a one-mode antenna subject to a white force signal, to the case of an arbitrary linear antenna subject to an arbitrary signal spectrum. The new result is derived by replacing the amplifier by its noise resistance, a quantity defined in terms of the amplifier noise spectral densities, and computing the energy dissipated in the noise resistance when a signal is applied. It is found that the optimally filtered SNR is less than or equal to $E_r/(kT_n)$, the energy dissipated in the noise resistance divided by Boltzmann's constant

times the amplifier noise temperature. The equality holds for a lossless system, for which all of the energy deposited in the antenna by the signal is eventually dissipated in the noise resistance. This result can be applied not only to gravitational wave antennas, but also to any linear instrument for which the SNR is the main figure of merit.

In practice, the sensitivity limit set by the electronic-amplifier noise temperature cannot be approached in resonant-mass antennas because of electrical losses in the electromechanical transducer. However, one may alternately view the antenna as a mechanical network, consisting of the main massive resonator (usually an aluminum cylinder) and one or more smaller impedance-matching resonators, followed by a mechanical amplifier, which includes the electromechanical transducer and the electronic amplifier. The losses in the mechanical network can be made small enough so that the sensitivity limit set by the mechanical-amplifier noise temperature (which is larger than the electronic-amplifier noise temperature) can be reached, at least for the case of a broadband signal and providing that a broadband impedance match is achieved between the main antenna mass and the mechanical amplifier. The case of a broadband signal is the case of most interest—almost all[6] research groups developing resonant-mass detectors optimize their instruments for detecting $\approx$1-msec broadband pulses, as would be produced by the gravitational collapse of solar-mass-sized objects. These signals are expected to be stronger than continuous sources, even allowing for the possibility of long averaging times with continuous signals.

A broadband impedance match must be achieved between the main resonator and the mechanical-amplifier noise resistance if the lossless sensitivity limit is to be reached. This is usually done by placing one or more additional resonators between the main resonator and the mechanical amplifier. The antenna will then have several normal modes. In Sec. III the impedance-matching problem is introduced by considering the limitations of a one-mode antenna, and then a lumped-element multimode antenna model is described. In Sec. IV the need for broadband impedance matching is explained in more detail in terms of the transfer function $Y_T(\omega)$, which relates the signal at the amplifier noise resistance to the applied gravity-wave force. It is found that for the system to be most tolerant to mechanical losses, the multimode matching network should be designed so that the transfer function $Y_T(\omega)$ is a broadband and flat function of frequency.

The techniques of network synthesis are applied in Sec. V to find a set of multimode matching networks that have a broadband and flat $Y_T(\omega)$. The realizability conditions on $Y_T(\omega)$ are stated, a family of maximally flat rational functions satisfying the realizability conditions is found, and network elements that realize the maximally flat $Y_T(\omega)$ are computed. The network-element values when expressed in dimensionless form depend on the number of modes and the value of the dimensionless noise resistance R_n, which is defined as the noise resistance divided by the impedance of the main mass at the center frequency. Plots of the resonator masses, resonant frequencies, and the bandwidth are given for one to eight modes and for $R_n = 10^{-4}$–10^{-7}. It is found that the bandwidth increases if either the number of modes or R_n increases. The tolerance of the maximally flat networks to mechanical losses is measured by computing the values of the resonator quality factors (Q's) that degrade the SNR by a factor of 2 from the lossless limit. Plots are given of the minimum tolerable Q's for the case where one of the resonator Q's is much lower than the others and for the case where all of the Q's are equal. The plots in Sec. V can be used as design charts. If the mechanical amplifier is given and one has some information about the mechanical Q's that can be achieved, then the plots can be used to find the number of modes that must be used to achieve a sufficiently broadband match so that the lossless limit is reached, and to find values for the resonator masses and spring constants.

The results are summarized in Sec. VI and their utility is illustrated by considering the future possibilities of the program at Stanford.

II. PROPERTIES OF THE SIGNAL-TO-NOISE RATIO

The sensitivity of resonant-mass antennas is limited by the noise temperature of the amplifier used to detect motions of the antenna. Giffard considered an antenna with one resonant mechanical normal mode, a passive linear electromechanical transducer, and a noisy linear electronic amplifier. He showed that when the signal is a δ-function force, the SNR is always less than or equal to the energy deposited in the antenna by the signal with the antenna initially at rest, divided by Boltzmann's constant times the amplifier noise temperature. (Giffard went on to show that, because the noise temperature of a linear amplifier is required by quantum mechanics to be greater than $\hbar\omega$, there is a fundamental limit set on the sensitivity of linear resonant-mass antennas.) For reasons that are considered in detail below, it is desirable to construct antennas with several normal modes, and thus extensions of Giffard's results must be considered.

In this section it is shown that Giffard's sensitivity limit applies to an arbitrary linear antenna subject to a δ-function force signal, and that *Giffard's limit is achieved by any lossless antenna.* The result is demonstrated as a specialization of a new theorem. The theorem provides a sensitivity limit for a generic instrument, consisting of a passive two-port network followed by a linear amplifier and subject to a signal with an arbitrary spectrum. For a signal that is not a δ function, a limit similar to Giffard's still holds, but the energy deposited must be calculated with the amplifier replaced by its noise resistance. In this case, also, the limit is achieved when the system is lossless.

A previous result generalizing Giffard's limit was found by Michelson and Taber,[7] who considered power matching between the dissipation of the first mass and the noise resistance, and were able to show that the sen-

sitivity limit applies to any antenna consisting of a (possibly lossy) resonant mass followed by a lossless passive two-port and subject to a δ-function force signal. Additional results are obtained here by focusing on the transfer function $Y_T(\omega)$, which relates the signal at the amplifier noise resistance to the force applied to the antenna. Further consideration of this quantity leads to the synthesis theory given in Sec. V.

The systems of interest are of the form shown in Fig. 1. The diagram could represent essentially any instrument for which the design figure of merit is the SNR. The dynamic variables indicated in the figure are force and velocity, but the discussion is, of course, unchanged if the system is electrical, electromechanical, or any other sort of linear system. In the Fourier-transform convention used here the force signal spectrum is

$$F(\omega)\equiv\int_{-\infty}^{+\infty}e^{-j\omega t}F(t)dt\ . \tag{1}$$

The signal is applied to a passive linear two-port in thermodynamical equilibrium at a temperature T. It is convenient to describe the two-port by its short-circuit admittance matrix $y_{ij}(\omega)$, which relates the port forces $f_1(\omega)$ and $f_2(\omega)$ to the port velocities $u_1(\omega)$ and $u_2(\omega)$:

$$\begin{aligned}u_1(\omega)&=f_1(\omega)y_{11}(\omega)+f_2(\omega)y_{12}(\omega)\ ,\\ u_2(\omega)&=f_1(\omega)y_{21}(\omega)+f_2(\omega)y_{22}(\omega)\ .\end{aligned} \tag{2}$$

The two-port is followed by a general noisy linear amplifier,[8] which contains force and velocity noise generators with stationary stochastic waveforms $f(t)$ and $u(t)$, and an ideal noiseless amplifier. The force noise generator is characterized by its spectral density

$$S_f(\omega)\equiv\int_{-\infty}^{+\infty}e^{-j\omega\tau}\langle f(t)f(t-\tau)\rangle d\tau\ , \tag{3}$$

and $S_u(\omega)$ is defined similarly. In general, the generators may be correlated, in which case the cross spectral density

$$S_{fu}(\omega)\equiv\int_{-\infty}^{+\infty}e^{-j\omega\tau}\langle f(t)u(t-\tau)\rangle d\tau \tag{4}$$

will be nonzero. It is simplest to imagine that the ideal amplifier has a zero input impedance, but this is not required since any (noiseless) impedance may be placed after the noise generators without affecting the SNR, or the SNR per unit bandwidth (defined below).

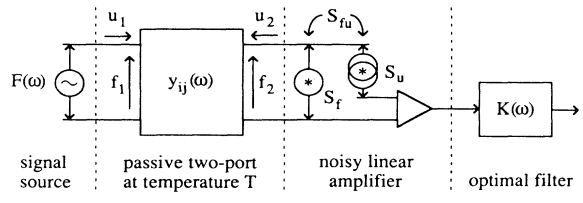

FIG. 1. A generic instrument. The variables f and u can represent force and velocity, voltage and current, or other dynamic variables. $F(\omega)$ is the Fourier transform of the signal, which is applied to a passive linear two-port at temperature T. The two-port is characterized by its short-circuit admittance matrix elements $y_{ij}(\omega)$. The noisy amplifier contains a force noise generator with spectral density S_f, a velocity noise generator with spectral density S_u, and a noiseless amplifier. The filter transfer function $K(\omega)$ is chosen to optimize the SNR.

The signal and noise output by the amplifier are processed by a filter than optimizes the SNR (Ref. 9). The filter's transfer function is

$$K(\omega)=\frac{e^{-j\omega t_0}u^*(\omega)}{S_n(\omega)}\ , \tag{5}$$

where $u(\omega)$ is the velocity signal at the ideal amplifier input, $S_n(\omega)$ is the total velocity noise spectral density at the ideal amplifier input, and t_0 is the time at which the SNR will be optimized by the filter. Because of the sophistication of modern digital filtering methods, it is safe to assume that a good approximation to the optimal filter can be implemented—this is certainly true for audio frequencies and below. The SNR, which is defined as the signal amplitude squared divided by the mean squared noise, is given at the output of the optimal filter and at time t_0 by

$$S/N=\frac{1}{2\pi}\int_{-\infty}^{+\infty}\frac{|u(\omega)|^2}{S_n(\omega)}d\omega\ . \tag{6}$$

The integrand of this expression is the SNR per unit bandwidth $\sigma(\omega)$.

Using Eq. (2), the integrand may be computed. With $S_{fu}(\omega)$ set to zero for the moment, the result is

$$\sigma(\omega)=\frac{|Fy_{21}|^2}{S_u+S_f|y_{22}|^2+2kT\,\mathrm{Re}(y_{22})}\ . \tag{7}$$

There are three noise terms in the denominator: the additive velocity noise, the force noise that drives the two-port output admittance y_{22}, and the thermal (Johnson-Nyquist) noise[10] due to losses in the two-port, which is given by twice Boltzmann's constant times the temperature times the real part of the output admittance.

It is fruitful to consider the circuit of Fig. 2, in which the amplifier has been replaced by its noise resistance

$$r_n\equiv(S_f/S_u)^{1/2}\ . \tag{8}$$

This circuit may be thought of as an energy analog for the noisy circuit of Fig. 1, because, as will be shown next, when a given signal is applied to the analog, the energy dissipated in r_n is closely related to the SNR for the circuit of Fig. 1 when it is subject to an identical signal.

The velocity $u_r(\omega)$ at the noise resistance is related to

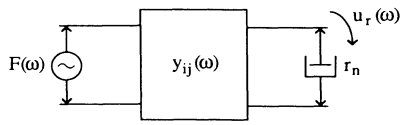

FIG. 2. A generic instrument with the noise amplifier replaced by r_n, the amplifier noise resistance. The relative velocity between the terminals of the noise resistance is denoted $u_r(\omega)$.

the applied signal force by the transadmittance $Y_T(\omega)$:

$$Y_T(\omega)\equiv u_r(\omega)/F(\omega)=\frac{y_{21}}{1+r_n y_{22}} . \tag{9}$$

The energy per unit bandwidth $e_r(\omega)$ dissipated in the noise resistance is given by

$$\begin{aligned} e_r(\omega)&=|F(\omega)Y_T(\omega)|^2 r_n \\ &=\frac{|Fy_{21}|^2}{|1+r_n y_{22}|^2} r_n \\ &=\frac{|Fy_{12}|^2}{1+r_n{}^2|y_{22}|^2+2r_n \mathrm{Re}(y_{22})} r_n , \end{aligned} \tag{10}$$

an expression remarkably similar to $\sigma(\omega)$, Eq. (7). It is now helpful to define the amplifier noise temperature T_n:

$$kT_n\equiv(S_f S_u)^{1/2} . \tag{11}$$

The basic sensitivity limit follows from writing the energy dissipated in r_n per unit bandwidth, divided by Boltzmann's constant times the noise temperature:

$$e_r(\omega)/(kT_n)=\frac{|Fy_{21}|^2}{S_u+S_f|y_{22}|^2+2kT_n\mathrm{Re}(y_{22})} . \tag{12}$$

This is identical to the expression for $\sigma(\omega)$, the SNR per unit bandwidth, in Eq. (7), except that T is replaced by T_n. Therefore, it follows that

$$\begin{aligned} &\sigma(\omega)<e_r(\omega)/(kT_n) \quad \text{if } T>T_n \text{ and } \mathrm{Re}(y_{22})\neq 0 , \\ &\sigma(\omega)=e_r(\omega)/(kT_n) \quad \text{if } T=T_n \text{ or } \mathrm{Re}(y_{22})=0 , \\ &\sigma(\omega)>e_r(\omega)/(kT_n) \quad \text{if } T<T_n \text{ and } \mathrm{Re}(y_{22})\neq 0 . \end{aligned} \tag{13}$$

[Note that $\mathrm{Re}(y_{22})\geq 0$ because the two-port is passive.] In all practical cases, the physical temperature T is greater than the noise temperature T_n, so $\sigma(\omega)$ is always less than the energy dissipated in r_n per unit bandwidth divided by kT_n, unless the two-port is lossless [$\mathrm{Re}(y_{22})=0$], in which case they are equal. The above relations can be integrated and, in most cases of interest, T_n is approximately constant over the range of frequencies where appreciable power is dissipated in r_n; so it may be brought outside the integral to yield

$$\begin{aligned} &S/N<E_r/(kT_n) \quad \text{if } T>T_n \text{ and } \mathrm{Re}(y_{22})\neq 0 , \\ &S/N=E_r/(kT_n) \quad \text{if } T=T_n \text{ or } \mathrm{Re}(y_{22})=0 , \\ &S/N>E_r/(kT_n) \quad \text{if } T<T_n \text{ and } \mathrm{Re}(y_{22})\neq 0 . \end{aligned} \tag{14}$$

In other words, *the signal-to-noise ratio is less than or equal to the total energy dissipated in the noise resistance, divided by Boltzmann's constant times the noise temperature, so long as T is greater than T_n; and the limit is achieved if the network is lossless.* Note that the energy dissipated in r_n is itself always less than or equal to the total energy deposited in the system by the signal, so the SNR is also less than or equal to the total energy deposited in the system, divided by Boltzmann's constant times the noise temperature, so long as T is greater than T_n. If the network is lossless, then all of the deposited energy must eventually be dissipated[11] in r_n, so then the SNR is equal to the total energy deposited in the system, divided by Boltzmann's constant times the noise temperature. The energy deposited must be computed with the amplifier replaced by its noise resistance.

Similar results may be obtained if $S_{fu}(\omega)$ is not zero. Then there is an extra noise term $2\,\mathrm{Re}(y_{22}S_{fu})$ in Eq. (7), and the amplifier must be replaced by its complex noise impedance

$$z_n\equiv\left[\frac{S_f}{S_u}-\left[\frac{\mathrm{Im}(S_{fu})}{S_u}\right]^2\right]^{1/2}+j\frac{\mathrm{Im}(S_{fu})}{S_u} , \tag{15}$$

which involves the imaginary part of the cross spectral density. The noise temperature becomes

$$kT_n\equiv\{S_f S_u-[\mathrm{Im}(S_{fu})]^2\}^{1/2} . \tag{16}$$

One can then show that

$$\begin{aligned} &\sigma(\omega)<e_z(\omega)/(kT_n) \\ &\qquad \text{if } T>T_n-\mathrm{Re}(S_{fu})/k \text{ and } \mathrm{Re}(y_{22})\neq 0 , \\ &\sigma(\omega)=e_z(\omega)/(kT_n) \\ &\qquad \text{if } T=T_n-\mathrm{Re}(S_{fu})/k \text{ or } \mathrm{Re}(y_{22})=0 , \\ &\sigma(\omega)>e_z(\omega)/(kT_n) \\ &\qquad \text{if } T<T_n-\mathrm{Re}(S_{fu})/k \text{ and } \mathrm{Re}(y_{22})\neq 0 , \end{aligned} \tag{17}$$

where $e_z(\omega)$ is the energy per unit bandwidth dissipated in z_n. Analogous expressions relate the integrated quantities.

The above results apply also to the case of an n-port, where the amplifier is connected to one port and the signal consists of several components with different waveforms which are applied to the other ports. The distributed interaction of a signal with a distributed network may be approximated as closely as one likes in this way. Thus, the SNR of a continuum elastic solid antenna interacting with a gravitational wave may be bounded by computing the total energy dissipated in the noise resistance by the signal, and it may be computed exactly in this way if the antenna is lossless.

If, as supposed by Giffard, the force signal is a δ function in time, then the energy deposited in each element depends only on its mass and its position, and so the total energy deposited in the antenna is the same whether or not the amplifier is replaced by its noise resistance. In this case, as was shown by Giffard for a one-mode antenna, the SNR is less than or equal to the energy deposited in the antenna divided by kT_n, even without replacing the amplifier by its noise resistance. If the antenna is lossless, the SNR is equal to the energy deposited in the antenna divided by kT_n; so Giffard's limit is achieved by any lossless antenna.

In practice, a lumped two-port gives a sufficiently accurate model of a resonant-mass antenna. One way to model an antenna is to include in the two-port the main antenna mass, any intermediate resonators intended to improve the matching, and the passive electromechanical transducer. In this case the two-port output vari-

ables are voltage and current, and the noisy amplifier is an electronic device (a dc SQUID, in most cases). For existing antennas the sensitivity limit set by the electronic amplifier noise temperature is not approached, mainly because the thermal noise of electrical losses in the transducer contributes substantially to the total noise. Alternatively, one may view the transducer and electronic amplifier together as a noisy linear mechanical amplifier and include only mechanical elements in the two-port. In this case, some existing detectors are in the lossless limit. For example, the Stanford 4 K, 4800 kg cryogenic antenna has a mechanical amplifier noise temperature of about 10 mK, and this is also the energy deposition required for a SNR of unity.

III. MULTIMODE RESONANT-MASS ANTENNAS

Given a mechanical amplifier with a certain noise temperature, the best antenna designs are those that will achieve the lossless sensitivity limit. Since realistic components are never perfectly lossless, a crucial question arises: How lossless is lossless enough? The answer to this question depends upon the design of the antenna. In particular, if the main antenna mass is impedance matched over a wide range of frequencies to the amplifier noise resistance, then the antenna can reach the lossless sensitivity limit even with relatively low Q values. In this section, the limitations of a one-mode antenna, which does not have broadband matching, are discussed, and multimode networks for broadband matching are introduced.

To understand the need for broadband matching, consider first the Q requirement of a one-mode antenna (Fig. 3). The mass m_1, spring constant k_1, and dissipation (force per unit velocity) d_1 are lumped elements chosen to model a mode of an elastic solid, which couples to gravitational radiation. Usually, the mass is a right cylindrical bar and we are interested in the lowest longitudinal mode. In this case, if the degree of freedom represented in the diagram is taken to be the distance from the center of mass to one end of the bar, then m_1 is given by the half the bar's mass and the signal is given by

$$F(\omega)=\frac{2}{\pi^2}m_1 L\omega^2 h(\omega)\ , \tag{18}$$

where L is the length of the bar and $h(\omega)$ is the Fourier transform of the metric perturbation of a favorably directed and polarized wave. The spring constant k_1 is fixed so that $(k_1/m_1)^{1/2}=\omega_1$ is the bar's resonant frequency, and the dissipation d_1 is chosen so that $Q_1=(\omega_1 m_1)/d_1$ is equal to the bar's quality factor. The thermal noise force spectral density is given by

$$S_{\rm th}=2kTd_1\ . \tag{19}$$

Since the thermal noise force generator appears in parallel with the amplifier force noise generator, it is clear that the sensitivity must become degraded whenever $S_{\rm th}$ is comparable to S_f. This implies that the quality factor must satisfy

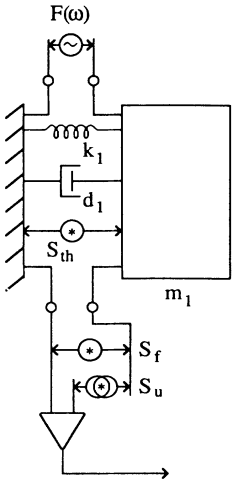

FIG. 3. Lumped-element model of a resonant-mass antenna with one normal mode. $F(\omega)$ is the Fourier transform of the applied force signal and k_1, m_1, and d_1 are the model's spring constant, mass, and dissipation (force per unit velocity). The thermal noise force spectral density is $S_{\rm th}$. The motion of the mass is monitored by a noisy mechanical amplifier, which consists of a force noise generator with spectral density S_f, a velocity noise generator with spectral density S_u, and a noiseless mechanical amplifier.

$$Q_1 \gg 2\frac{T}{T_n}\frac{\omega_1 m_1}{r_n} \tag{20}$$

if the lossless limit is to be achieved. The temperature ratio is about 400 for present cryogenic detectors (4 K/10 mK), and the ratio of impedances $(\omega_1 m_1)/r_n$ is in the range 10^5–10^7 for present systems. Thus, for a one-mode antenna to be in the lossless limit, very high mechanical quality factors are required—at least 10^8 for present parameters. Since $\sigma(\omega)$ for a lossless system is proportional to the energy per unit frequency dissipated in the noise resistance, the fractional bandwidth $\Delta f/f$ of a lossless one-mode system is given by Q^{-1} with the amplifier replaced by r_n:

$$\Delta f/f=\frac{r_n}{\omega_1 m_1}\ . \tag{21}$$

This is equal to 10^{-5}–10^{-7} for present systems. As will be explained in more detail in the next section, systems with small bandwidths in the lossless limit will always require high mechanical quality factors. The connection between bandwidth and Q requirements has been emphasized by Michelson and Taber.[7]

The small bandwidth of a one-mode system stems from an impedance mismatch. The noise resistance of practical mechanical amplifiers is much smaller than the impedance of the antenna mass. The first cryogenic antenna built in Stanford[12] introduced broadband mechanical resonant matching. A second resonator, much lighter than the main antenna mass, was attached to the face of the bar, and the mechanical amplifier measured the distance between the face of the bar and the addi-

tional resonator. This two-mode arrangement can provide a much larger bandwidth than a one-mode design. Richard[13] has discussed systems with more than two modes, and has shown that even more bandwidth can be obtained. The network synthesis results, presented in Sec. V, detail the Q requirements of a class of optimal multimode systems; they are much less severe than for one-mode designs. Other methods for achieving a broadband impedance match have been suggested, including a lever[14] and tapered transmission lines.[15]

The general m-mode lumped element model, as given by Richard, is shown in Fig. 4. There are now m masses, m springs, m dissipative elements (with m associated thermal noise sources), and m resonant frequencies ω_i and quality factors Q_i:

$$\omega_i \equiv (k_i/m_i)^{1/2}, \quad Q_i \equiv \frac{\omega_i m_i}{d_i}, \quad i = 1,2,\ldots,m \ . \tag{22}$$

As for a one-mode system, if the first resonator takes the form of a cylindrical bar, then m_1 is equal to half the bar's mass, and the force signal is given by Eq. (18). The higher normal modes of the bar and its zero frequency mode, and any other parasitic modes that may be present in the system, are not included in the model. This is an acceptable approximation if the neglected modes are far enough away from the passband of the detector. Also, the coupling of the gravitational wave to the secondary masses, which are much smaller than m_1, is neglected.

To make a full analysis of a particular multimode system, it is necessary to compute the admittance matrix elements $y_{22}(\omega)$ and $y_{21}(\omega)$, substitute them into the integrand of Eq. (7) to find $\sigma(\omega)$, and integrate to find S/N. [In general, the correlation noise term $2\mathrm{Re}(y_{22}S_{fu})$ must be included.] In principle, this is a straightforward network analysis problem. Numerical results have been given by several authors,[16] sometimes showing the effect of variations of a particular parameter. The design problem, in contrast with the analysis problem, requires the study of the whole class of multimode systems to find those that are optimal according to a certain criterion. This might be addressed by numerical optimization, but it becomes difficult to fully explore the possibilities when the number of parameters is large. An alternative, considered in Sec. V, is to use the methods of network synthesis, which, in some circumstances, allow one to compute the network component values that will produce some desired behavior. It is still important to have a numerical model at hand to study those questions which cannot be addressed by synthesis. A compact numerical algorithm for analyzing the general multimode system of Fig. 4 is presented in Appendix A.

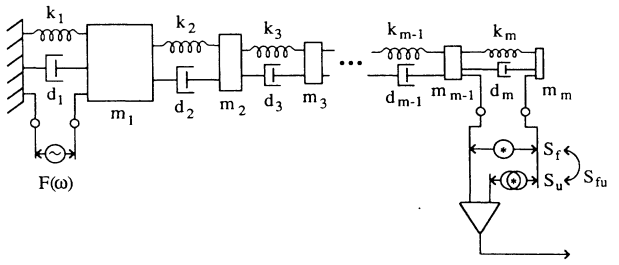

FIG. 4. Lumped element model of an antenna with m normal modes. There are m masses, m springs, and m dissipative elements. The motion of the last mass relative to the next to the last mass is monitored by a noisy mechanical amplifier.

For the sake of the discussion to follow, it is useful to place some restrictions on the noisy amplifier model, which has so far been general. A number of authors have discussed the noise models of mechanical amplifiers.[5,17] For superconducting variable-inductance transducers coupled to SQUID amplifiers,[18] the force noise is thermal noise from electrical losses and the velocity noise is the SQUID flux noise referred to the transducer input. The force and velocity noise spectral densities are both slowly varying functions of frequency near 1 kHz, and they are uncorrelated because they originate in separate mechanisms. The noise model for these devices must include an input impedance consisting of the reactance of the magnetic spring and the reactance of the mass of the superconducting diaphragm. These components must be placed before the noise sources. It is possible to use a noise model in which the input components are omitted, but then the noise generators would become correlated. In this paper it will be assumed that the mechanical amplifier noise generators are uncorrelated, and it will be assumed that if any input components must be placed before the noise generators, then they can be absorbed in the last mass and spring, m_m and k_m, of the matching network. It will also be assumed that the noise temperature T_n and noise resistance r_n are constant functions of frequency, to a good approximation within the frequency range where $\sigma(\omega)$ is not negligible.

IV. OPTIMAL DESIGN FOR PULSE DETECTION

In this section it is argued that the best multimode designs for pulse detection are those for which the transfer function $Y_T(\omega)$ is a broadband and flat function of frequency. A network will be judged best if it is most tolerant to losses, in the sense that the lossless sensitivity limit can be reached with the lowest possible resonator Q values. Of course, it is also required that the lossless SNR be as large as possible. The lossless SNR of a given network will depend on the signal spectrum, so it is necessary to assume a definite spectrum to proceed.

A simplification results if, following Giffard, one idealizes the broadband pulse as a white force spectrum, corresponding to a strain spectrum $h(\omega)$ that varies as ω^{-2}. This idealization need only apply approximately, and only over the frequency range where $\sigma(\omega)$ is appreciable, since a given design will be insensitive to $F(\omega)$ outside this range. If the interaction of the gravitational wave with the small matching resonators is neglected, that the energy E deposited in the multimode model by the force impulse is given by

$$E=\frac{|F(\omega_c)|^2}{2m_1}, \tag{23}$$

where ω_c is the center frequency about which $\sigma(\omega)$ is appreciable. Thus, for a white force spectrum, the SNR in the lossless limit depends only on the properties of the main resonator. Only loss tolerance need be considered when designing the matching resonators.

According to Eq. (18), the deposited energy is proportional to m_1L^2, so, to increase the lossless SNR, the bar (or other object which serves as the main resonator) should be as long and massive as possible. Unfortunately, once the center frequency and material are chosen, the length of the bar is fixed, since the resonant frequency ω_1 is given by the longitudinal speed of sound divided by twice the length, and the center frequency ω_c will always turn out to be close to the resonant frequency.

The function of the matching resonators is to improve the performance of the system when the quality factors Q_i take finite values. A useful viewpoint is that an optimal design is one which achieves the lossless limit with the lowest possible values of the resonator Q's. A tractable problem is to set all of the resonator Q's equal to infinity except Q_1, and to find those networks which achieve the lossless limit with the lowest possible value of Q_1. A satisfactory solution to the problem of finding multimode networks that are tolerant to losses in any resonator seems to result because it is found that networks designed to be tolerant to losses in the first resonator are still more sensitive to losses in the first resonator than to losses in the other resonators. Thus, if high Q values are equally difficult to achieve in each of the resonators, one should choose the design that allows the lowest possible Q for the first resonator. In Sec. V the minimum tolerable Q's for maximally flat networks will be given; in every case it is Q_1 that must be highest.

Usually the simplest way to include the effects of the thermal noise of losses is to compute the real part of the output admittance y_{22}, as indicated in Eq. (7). An alternative method is to explicitly include in the model the thermal noise sources associated with each d_i (the dissipative element that gives rise to Q_i), and to compute the transfer functions needed to find the noise at the amplifier input due to each thermal noise source. When the computations for multimode networks are done in this way, one finds that, to an excellent approximation, the d_i themselves may be neglected, so long as their associated noise generators are retained. Thermal noise in the networks synthesized in Sec. V may be accurately treated within this approximation.

With all of the d_i equal to zero, but with the thermal noise of d_1 included, the SNR is given by

$$S/N=\frac{1}{2\pi}\int_{-\infty}^{+\infty}\frac{|F(\omega)y_{21}|^2}{S_u+S_f|y_{22}|^2+2kTd_1|y_{21}|^2}d\omega . \tag{24}$$

Noting that the admittance matrix elements describe a lossless network, this can be rewritten as

$$S/N=\frac{1}{2\pi}\frac{|F(\omega_c)|^2r_n}{kT_n}\times\int_{-\infty}^{+\infty}|Y_T(\omega)|^2\frac{1}{1+2\frac{T}{T_n}r_nd_1|Y_T(\omega)|^2}d\omega , \tag{25}$$

where Y_T is the transadmittance defined by Eq. (9), and $F(\omega)$ is equal to $F(\omega_c)$ where the integrand is appreciable. If the dissipation is small, then the fraction in the integrand may be expanded to yield

$$S/N=\frac{1}{2\pi}\frac{|F(\omega_c)|^2r_n}{kT_n}\times\int_{-\infty}^{+\infty}\left[|Y_T|^2-2\frac{T}{T_n}r_nd_1|Y_T|^4+\cdots\right]d\omega . \tag{26}$$

The integral of the first term must give the lossless SNR, so $|Y_T|^2$ is proportional to the lossless $\sigma(\omega)$, and comparison with Eq. (23) implies

$$\int_{-\infty}^{+\infty}|Y_T|^2d\omega=\frac{\pi}{m_1r_n} . \tag{27}$$

The integral of $|Y_T|^2$ is a constant independent of the masses and frequencies of the matching resonators, while the integral of $|Y_T|^4$ determines how large d_1 (or how small Q_1) can be before the SNR is degraded. Thus, a multimode system will be most tolerant to dissipation in the main resonator if the matching resonators are designed to minimize the integral of $|Y_T|^4$. Since the integral of $|Y_T|^2$ is fixed, this can only be done by making $|Y_T|^2$ broadband and smooth; any peaks in $|Y_T|^2$ will contribute unnecessarily to the integral of $|Y_T|^4$. When $|Y_T|^2$ is broadband there is a broadband impedance match between the first resonator mass and the noise resistance.

If $|Y_T|^2$ is a square bandpass function with fractional bandwidth $\Delta f/f$ then Eqs. (25) and (27) together imply that the dissipation in the main resonator will be negligible if

$$Q_1\gg\frac{T}{T_n}\frac{1}{\Delta f/f} . \tag{28}$$

This is consistent with Eq. (20) for the one-mode case. The essential advantage of multimode systems is that the fractional bandwidth can be large.

The requirements that the integral of $|Y_T|^4$ be minimized while the integral of $|Y_T|^2$ is kept constant are not, however, the only conditions that $|Y_T|^2$ must satisfy. Because $|Y_T|^2$ is the magnitude of a transfer function of a two-part network, it must also satisfy certain realizability conditions, to be discussed in the next section. It is not clear how to solve exactly the problem of minimizing the integral of $|Y_T|^4$ while also satisfying the other conditions, but the problem can be solved

approximately by choosing $|Y_T|^2$ from a family of maximally flat bandpass functions that satisfy the realizability conditions.

V. NETWORK SYNTHESIS

The multimode design problem has now been reduced to a specification on a transfer function of a lossless two-port terminated at one end by a resistor. A well-developed synthesis theory exists for this circumstance, that often permits one to compute component values that generate a specified behavior. For the present problem, the method of Cauer and Guillemin[19] can be applied to find multimode networks with flat $Y_T(\omega)$.

To make contact with the existing theory,[20] it is helpful to go over to an electrical analog circuit, shown in Fig. 5(a). The classical analog is used in which voltage is analogous to force, current to velocity, inductance to mass, and capacitance to inverse spring constant. In Fig. 5(b) the amplifier has been replaced by its noise resistance and the output components have been rearranged. The network is now recognizable as a lossless ladder, a network with alternating series and shunt branches that are lossless.

Network synthesis proceeds in three stages. First, realizability conditions on the desired network functions are found; these conditions specify the class of rational functions that may be used for a particular network function. If it is required that the network be implemented in a particular topology (a ladder, for example) or with particular components (no transformers, inductors and resistors only, etc.), then there will be additional realizability conditions. Next, it is necessary to find a rational function that satisfies the realizability conditions and also satisfies whatever performance requirements are at hand; this is called the approximation problem. Finally, there is the synthesis problem itself, in which a circuit is found and component values are calculated

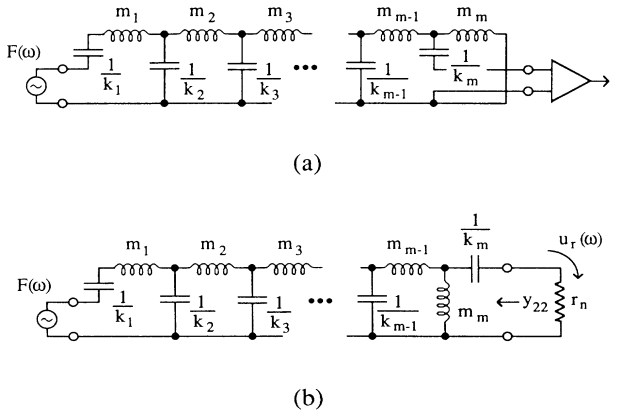

FIG. 5. (a) Electrical-analog circuit for a multimode antenna with m normal modes. The masses m_i correspond to inductances, and the spring constants k_i correspond to inverse capacitances. (b) The electrical analog with the amplifier replaced by its noise resistance and with the last mass and spring rearranged. The circuit is in the form of a lossless ladder.

that realize the chosen rational function.

If the elements y_{ij} in Fig. 2 represent any linear lumped passive two-port, and r_n is a specified resistance, then for the transadmittance $Y_T(s)$ to be realizable it must be in the form

$$Y_T(s)=\frac{P(s)}{Q(s)}\ , \tag{29}$$

where P and Q are polynomials with real coefficients, and all of the zeros of $Q(s)$ are in the left half-plane, with none on the $j\omega$ axis (s is the complex frequency variable, $s\equiv\rho+j\omega$) (Ref. 21). If the two-port is a ladder, then the zeros of $P(s)$ (which are known as the zeros of transmission) can only occur at zeros of the series branch admittances or poles of the shunt branch admittances.[22] For a lossless ladder, these are on the $j\omega$ axis, so the zeros of $P(s)$ are restricted to the $j\omega$ axis. The particular lossless ladder of Fig. 5(b) has just three finite zeros of transmission, all at $s=0$, due to k_1, m_m, and k_m. (For the case of one mode, there is one zero of transmission at $s=0$.) Thus, for the present example, realizable rational functions $Y_T(s)$ must have poles only in the left half plane and must have just three finite zeros, all at the origin. Note that since the polynomial coefficients are real, the s-plane poles must have reflection symmetry about the real axis. The magnitude function $|Y_T(\omega)|^2$ must have a sixfold zero at the origin, and, since its analytic continuation in the s plane is given by $Y_T(s)Y_T(-s)$, its poles in the s plane must have reflection symmetry about both the real and the imaginary axes.

These realizability conditions are necessary. Generally, in network synthesis the sufficiency of realizability conditions is demonstrated by the synthesis procedure itself. For this case, the synthesis procedure will show that for a particular value of r_n, any Y_T with the analytic structure given above can be synthesized up to a constant factor in the form of Fig. 5(b). Thus, the conditions given above are sufficient for realization up to a constant factor. Once the poles and r_n are specified, the synthesis procedure results in a unique value for all of the masses and springs. However, what one wishes to do here is to solve the synthesis problem with both r_n and m_1, the main resonator mass, specified. Stating sufficient realizability conditions for such a constrained synthesis problem is difficult. One might think that the normalization requirement (27) is the additional condition required, but this is not the case—Eq. (27) is only a necessary condition for the constrained problem. The constrained problem can be avoided by carrying out the synthesis up to a constant for a one-parameter family of Y_T that satisfy the known necessary conditions. If for some value of the parameter one finds that m_1 takes the desired value, then Y_T with this value of the parameter is a solution to the constrained problem. Once the value of the parameter is known, the constant factor can be found from Eq. (27), if it is needed.

It is simplest to solve the approximation problem in terms of the magnitude function $|Y_T(\omega)|^2$. Because the critical frequencies have quadrantal symmetry, the magnitude function is a function of ω^2, and it has the

form

$$|Y_T(\omega)|^2 \propto \frac{\omega^6}{\sum_{i=0}^{2m} a_i \omega^{2i}} , \tag{30}$$

where the a_i are real constants. The synthesis will show that the order of the denominator of Y_T is equal to the number of reactive elements in the network. Since this is equal to twice the number of modes m, the order of the denominator of the magnitude function should be $4m$.

To make the multimode system tolerant to losses, the magnitude function $|Y_T(\omega)|^2$ should be broadband and smooth. This requirement can be satisfied in a qualitative way by setting as many derivatives with respect to ω as possible equal to zero at the center frequency ω_c. Approximations of this kind are called maximally flat and are widely used,[23] in part because they usually lead to polynomials that are easy to factor. In Appendix B a maximally flat approximation of the form of Eq. (30) is derived. The result, which has all derivatives up to and including order $2m-1$ equal to zero at $\pm\omega_c$, is

$$|Y_T(\Omega)|^2 \equiv \frac{H^2(\delta,1)\Omega^2}{(1-\Omega^2)^2+\Omega^2\delta^2}, \quad m=1 ,$$
$$|Y_T(\Omega)|^2 \equiv \frac{H^2(\delta,m)\Omega^6}{(1-\Omega^2)^{2m}+\Omega^6\delta^{2m}}, \quad m=2,3,\ldots , \tag{31}$$

where Ω is the dimensionless frequency variable $\Omega \equiv \omega/\omega_c$, and the solutions depend on a dimensionless parameter δ, which characterizes the fractional bandwidth. The parameter δ will be used to satisfy the constraint mentioned above. For one mode, $|Y_T(\Omega)|^2$ takes the form of a resonance curve with $\delta = Q^{-1}$. When δ is much less than unity, the poles in the S plane (the dimensionless s plane, $S \equiv s/\omega_c$) are located on two circles of diameter δ, one centered on $S=j$ and one centered on $S=-j$. The undetermined overall constant H will depend on the number of modes m and the value of δ. Figure 6 shows an example of a maximally flat magnitude function together with the pole positions. When m is large the maximally flat functions have nearly ideal bandpass characteristics.

The synthesis proceeds from $Y_T(s)$, which may be derived uniquely from $|Y_T(\omega)|^2$ by making the replacement $s=\omega/j$ and assigning three of the zeros and all of the left half-plane poles to $Y_T(s)$. Then the numerator polynomial $P(s)$ and the denominator polynomial $Q_{\text{even}}(s)+Q_{\text{odd}}(s)$ are divided by the even part of the denominator:

$$Y_T(\omega) = \frac{y_{21}}{1+r_n y_{22}}$$
$$= \frac{P(s)/Q_{\text{even}}(s)}{1+Q_{\text{odd}}(s)/Q_{\text{even}}(s)} . \tag{32}$$

The ratio of the odd to the even part of a polynomial with all its zeros in the left half-plane is always a realizable lossless driving point function.[24] Therefore, the identification

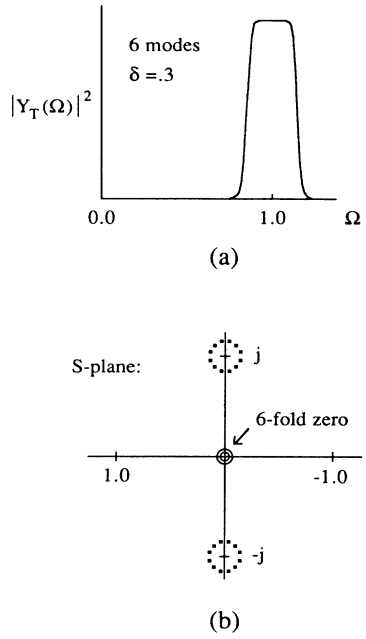

FIG. 6. The maximally flat magnitude function for six modes and a bandwidth parameter $\delta=0.3$ (a) plotted as a function of the dimensionless frequency Ω; (b) the poles and zeros in the dimensionless complex frequency plane. $|Y_T(\Omega)|^2$ is proportional to the signal-to-noise ratio per unit bandwidth when the applied force spectrum is white. For 6 modes there are 24 poles situated in two nearly circular patterns. For any number of modes greater than one there is a sixfold zero at the origin.

$$y_{22}(s) = \frac{1}{r_n}\frac{Q_{\text{odd}}(s)}{Q_{\text{even}}(s)} \tag{33}$$

can be made, and the canonical ladder realizations of lossless driving point functions due to Cauer[25] will always permit y_{22} to be realized in the form shown in Fig. 5(b). When y_{22} is realized in this form, y_{21} will automatically have the correct zeros (the same zeros as Y_T) and the correct poles (the poles of y_{22}). Thus, realization of y_{22} in the form shown in Fig. 5(b) realizes Y_T as well, up to a constant factor.

The Cauer synthesis of lossless driving point functions is based on a continued-fraction expansion. The reciprocal of the admittance y_{22} in Fig. 5(b) can be expressed, starting from the right, as the impedance of the first series branch plus the parallel sum of the impedance of the first shunt branch and the remaining impedance to the left, which itself is given by the impedance of the second series branch plus the parallel sum of the impedance of the second shunt branch and the then remaining impedance. Expanding y_{22} in this way leads to a continued fraction

$$y_{22}=\cfrac{1}{\cfrac{k_m}{s}+\cfrac{1}{\cfrac{1}{sm_m}+\cfrac{1}{sm_{m-1}+\cfrac{1}{\cfrac{s}{k_{m-1}}+\ddots\;sm_2+\cfrac{1}{\cfrac{s}{k_2}+\cfrac{1}{sm_1+\cfrac{1}{\cfrac{s}{k_1}}}}}}}}} \quad . \tag{34}$$

An expansion of Eq. (33) in this form can be accomplished by synthetic division.[26] In general, the expansion can be in terms of s or $1/s$; to yield the circuit of Fig. 5(b), the first two steps of the expansion are done in $1/s$ and the remainder are done in s. The resulting terms can then be identified with the terms of Eq. (34) to find the values of the masses and springs.

Figures 7 and 8 detail the networks that result for a range of values of r_n and for one to eight modes. It is convenient to define a dimensionless noise impedance R_n by dividing r_n by the impedance of the first mass at the center frequency:

$$R_n \equiv \frac{r_n}{\omega_c m_1} \quad . \tag{35}$$

This quantity gives a measure of the intrinsic mismatch between the main resonator and the amplifier, its value for present systems is in the range 10^{-5}–10^{-7}.

To solve the constraint, the value of δ that leads to a desired value of m_1 for each value of r_n must be found. Actually, for a given solution, all of the impedances may be rescaled without changing δ, so δ depends only on the impedance ratio R_n. The values of the bandwidth parameter δ that correspond to particular values of R_n are given in Fig. 7. For one mode, the bandwidth parameter is equal to R_n [recall Eq. (21)], and when there are many models it tends towards unity. Thus, an impedance match can be achieved over a very wide band if many modes are used. Note that for a given number of modes, the bandwidth is smaller for smaller values of R_n, and it increases very slowly beyond three modes.

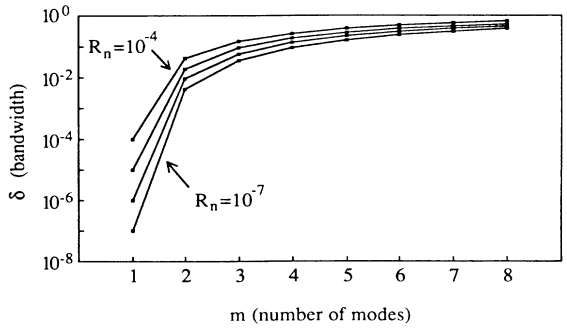

FIG. 7. The bandwidth parameter δ for maximally flat networks plotted as a function of the number of modes m. The four curves are for different values of the dimensionless noise resistance: $R_n=10^{-4}$, 10^{-5}, 10^{-6}, and 10^{-7}.

The masses and frequencies for maximally flat networks are given in Fig. 8 in terms of the dimensionless masses $M_i \equiv m_i/m_1$ and the dimensionless frequencies $\Omega_i \equiv \omega_i/\omega_c$. M_1 is always equal to 1 by definition, and Ω_1 is always very close to 1. As the number of modes increases, the value of the last mass becomes approximately equal to R_n. The dimensionless frequencies do not differ from unity by more than a factor of 2.

The numerical model of Appendix A may now be used to measure the tolerance of the maximally flat networks to finite Q values. If, as discussed in Sec. IV, the d_i may be neglected as long as the thermal noise sources are retained, then the SNR will depend on Q_i/T, and not on Q_i and T separately. For a given signal, given masses and springs, and given r_n, the SNR can then be expressed as a function of T_n and the scaled quality factors:

$$\tilde{Q}_i \equiv \frac{T_n}{T} Q_i \quad . \tag{36}$$

One way to characterize the loss tolerance is to find for each value of i the value of $\tilde{Q}_i$, which reduces the SNR by a factor of 2 from the lossless value, with all of the other $\tilde{Q}_j$ $(j \neq i)$ set to infinity. These minimum tolerable $\tilde{Q}_i$ values are denoted $\tilde{Q}_i^{\min}$, and are plotted in Fig. 9. For one mode, $\tilde{Q}_1^{\min}$ is given approximately by R_n^{-1}, as is suggested by Eq. (28). For more modes, the bandwidth increases and the $\tilde{Q}_i^{\min}$ tend approximately towards unity. Thus, the tolerance to losses does indeed increase as the impedance matching becomes more broadband. In all cases, the first resonator is more sensitive to Q degradation than the following resonators, which suggests that the method used here—design for greatest loss tolerance in the first resonator—is appropriate. Another way to measure the Q tolerance is to find the $\tilde{Q}_i$ value that degrades the SNR by two with all of the $\tilde{Q}_i$ equal. This quantity, denoted $\tilde{Q}^{\min}$, is plotted in Fig. 10. The curves are nearly flat beyond three modes; the $R_n=10^{-7}$ curve tends to $\tilde{Q}^{\min} \approx 30$ and the $R_n=10^{-4}$ curve tends to $\tilde{Q}^{\min} \approx 20$. The curves will eventually begin to rise as the number of modes in-

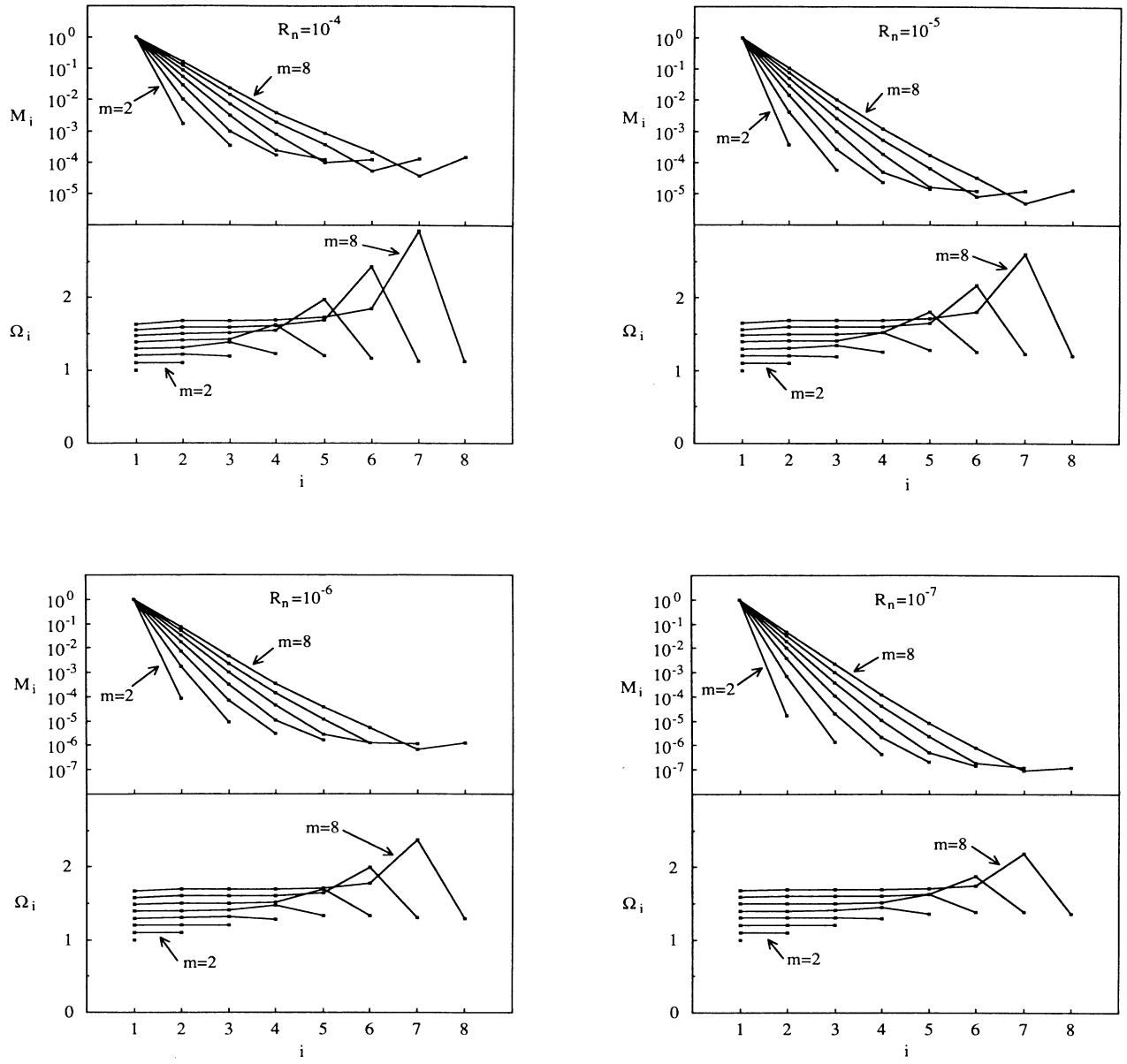

FIG. 8. The dimensionless masses M_i and dimensionless resonator frequencies Ω_i for maximally flat networks, for from one to eight modes, and for $R_n = 10^{-4}$, 10^{-5}, 10^{-6}, and 10^{-7}. The Ω_i curves have been staggered for clarity. The $m=2$ curve is offset by 0.1, the $m=3$ curve is offset by 0.2, and so forth.

creases because the fractional bandwidth does not increase beyond unity, but each additional resonator introduces more thermal noise.

Note that the numerical model of Appendix A does not use the approximation that the d_i are set to zero. According to this approximation, the results in Figs. 9 and 10 should not depend on T/T_n if its value is large enough. It is found that the results do not vary by more than 10% as long as $T/T_n > 10$; so it may be concluded that neglecting the d_i is a good approximation for computing the loss tolerance of these networks if $T/T_n > 10$. This condition is satisfied in practice.

Figures 7–10 may be used as a set of design charts for multimode antennas. First, the antenna mass and center frequency are chosen, and R_n and T_n are computed for the available mechanical amplifier. Next, the Q values that can be achieved are estimated, and Fig. 9 or 10 is used to find the number of modes that must be used to make the losses negligible. Figure 9 is used if it is expected that one of the resonators will have a much lower Q than the others, and Fig. 10 is used if all of the Q values are expected to be equal. Once the number of

modes is known, the resonator masses and frequencies can be taken from Fig. 8 and the bandwidth that will result can be taken from Fig. 7.

It is believed that the maximally flat networks are very close to the most loss tolerant designs possible within the multimode model. With more complicated acoustic networks that would allow the zeros of transmission to be placed anywhere along the imaginary axis, it would be possible to achieve greater bandwidth, for a given number of reactive components, than the networks used here allow. However, the main features of the maximally flat multmode networks are expected to be general: the bandwidth starts at R_n, and increases rapidly as the number of modes goes from one to three, and then approaches unity slowly as the number of modes increases further; small values of R_n require more modes for a given bandwidth than larger values; the final mass tends towards $\approx m_1 R_n$; the minimum tolerable Q values go from $(T/T_n)R_n^{-1}$ for one mode to $\approx T/T_n$ for many modes.

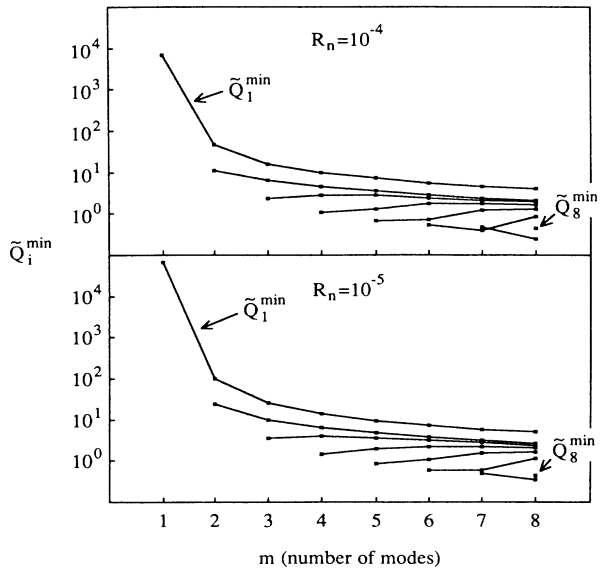

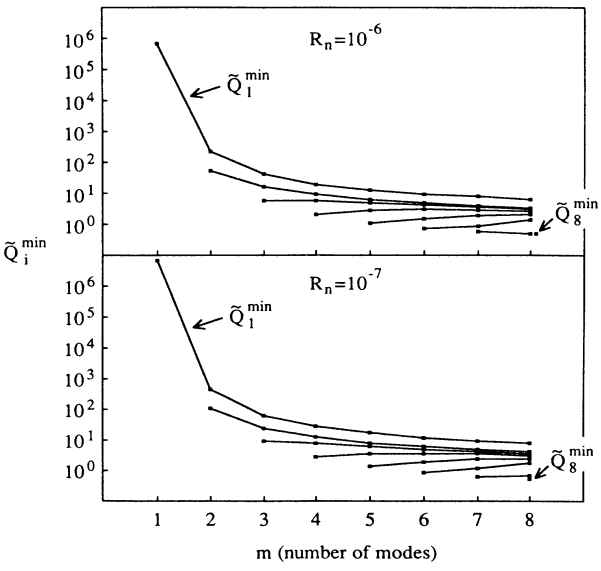

FIG. 9. The minimum tolerable scaled resonator quality factors for the case where one of the resonator quality factors is much less than the others. $\tilde{Q}_i^{min}$ is defined as the value of the scaled quality factor $\tilde{Q}_i$ that degrades the SNR by two from its lossless value, when the other $\tilde{Q}_j$ $(j \neq i)$ are infinite. The main resonator is $i=1$.

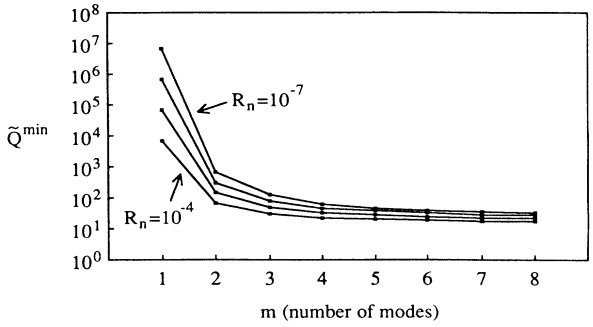

FIG. 10. The minimum tolerable scaled resonator quality factors for the case where the quality factors of the different resonators are all equal. $\tilde{Q}^{min}$ is defined as the value of the scaled quality factor $\tilde{Q}_i$ that degrades the SNR by two from its lossless value, when all of the $\tilde{Q}_i$ are set to the same value.

VI. SUMMARY

This paper has tried to address those design problems which are common to the various research groups now engaged in the development of resonant-mass gravitational wave antennas. Under very general conditions, all resonant-mass antennas, and indeed all linear instruments, are subject to the limitation that the optimally filtered signal-to-noise ratio is less than or equal to the energy dissipated in the amplifier noise resistance divided by Boltzmann's constant times the amplifier noise temperature: $S/N \leq E_r/(kT_n)$. Lossless systems always achieve this sensitivity limit, and the energy dissipated in the noise resistance of a lossless system is equal to the energy deposited in the system by the signal. The design problem for resonant-mass antennas can be thought of as having two aspects: the lossless SNR should be large, and the actual SNR should approach the lossless limit as closely as possible.

If the problem of pulse detection is to be treated, and one idealizes the pulse as a force δ function, then an important simplification results because the energy deposited in the antenna will depend only on the mass distribution. If a lumped element model of the antenna is used and one neglects the interaction of the gravitational wave with masses other than the main resonator, then the energy deposited depends only on the mass and shape of the main resonator, so the SNR in the lossless limit depends only on the main resonator and the amplifier noise temperature. The system can be made

tolerant to the losses actually present by using additional components to provide a broadband match between the main resonator and the amplifier noise resistance. In practice, the lossless limit imposed by the electronic-amplifier noise temperature cannot be approached with present technology because of electrical losses. However, if the electronic amplifier and electromechanical transducer are modeled together as a mechanical amplifier, then the lossless limit imposed by the mechanical-amplifier noise temperature is accessible.

If the acoustic network used to match the main resonator to the mechanical amplifier noise resistance has the simple mass-spring-mass-spring configuration, then the multimode lumped-element model of Fig. 4 results. For a given mechanical amplifier and a given main resonator, the design problem amounts to finding values of the masses and springs of the matching resonators that allow the system to most closely approach the lossless sensitivity limit when the mechanical quality factors take on realistic values. It was argued in Sec. IV that for maximum loss tolerance the transfer function $Y_T(\omega)$, which relates the velocity at the noise resistance to the applied force signal, should be a broadband and flat function of frequency.

With the desired behavior of the network function $Y_T(\omega)$ specified, the techniques of network synthesis can be used to find corresponding values for the masses and springs. The synthesis consists of three steps: first, realizability conditions are found; then a rational function with the specified behavior and satisfying the realizability conditions is found; finally, the component values, which realize the network function, are computed. A rational function of the maximally flat type satisfying the realizability conditions was used in Sec. V to synthesize a family of loss-tolerant multimode networks.

The most important properties of these networks are summarized in Table I, where the one-mode and many-mode behaviors are compared. The fractional bandwidth of a one-mode system is given by the dimensionless noise impedance R_n, which is always much less than 1, while for a many-mode system the fractional bandwidth approaches unity (see Fig. 7 for details). As a consequence, the minimum Q that can be tolerated without degrading the SNR from the lossless value is smaller by a factor of R_n for a many-mode system than for a one-mode system (Figs. 9 and 10). The final mass of a many-mode system is also a factor of R_n smaller than the main mass (Fig. 8). Most of the improvement to be gained in going from one mode to many modes is realized with a small number of modes; in most cases one would not have reason to use more than about three modes.

TABLE I. Summary of the properties of the maximally flat multimode networks, for one mode and for many modes. The entry for the minimum tolerable Q in the many mode case is approximate—there is a numerical factor of 1–8 for the case where one Q is much less than the others, and a factor of 20–30 for the case where all the Q values are equal.

	One mode	Many mode
Fractional bandwidth	R_n	1
Minimum tolerable Q	$\frac{T}{T_n}\frac{1}{R_n}$	$\frac{T}{T_n}$
Final mass	m_1	$m_1 R_n$

The future development of the program at Stanford can be used to illustrate the utility of the results of this paper. In the next generation, it may be possible to build a mechanical amplifier with a noise temperature $T_n = 10\ \mu$K, and a dimensionless noise impedance R_n of about 10^{-6} (for an antenna mass m_1 of 2000 kg and a center frequency of 1 kHz). Even at low dilution refrigerator temperatures ($T \approx 10$ mK, $T/T_n \approx 10^3$) a one-mode system would require an impossibly high Q of about 10^9 (Fig. 10). For a two-mode system, assuming that the Q values of the main and secondary resonators are equal, Fig. 10 implies that Q's of only 3×10^5 are needed at 10 mK. Typically, mechanical Q's of at least several million are achieved, so such an antenna could be operated at higher dilution refrigerator temperatures (≈ 100 mK). Even with many modes, it would be difficult to operate at 4 K ($T/T_n = 4\times10^5$), since, according to Fig. 10, Q's of about 10^7 would be required. Thus, in the next generation, limitations due to mechanical losses are not very severe if the temperature is well below 4 K. A 2000-kg antenna operating at the mechanical amplifier sensitivity limit with $T_n = 10\ \mu$K can detect a 1-msec pulse of dimensionless amplitude 3×10^{-20} with an SNR of unity.

For a future quantum limited antenna ($T_n = 40$ nK at 1 kHz), the Q requirements are more difficult to satisfy. For $R_n = 10^{-6}$ and $T = 10$ mK ($T/T_n = 2.5\times10^5$), Fig. 10 implies that a two-mode antenna must have Q's of 8×10^7, a three-mode antenna must have Q's of 2×10^7, and a six-mode antenna requires Q's of 8×10^6. The large aluminum antenna ($m_i = 1100$ kg) constructed by the Rome group[27] has a Q of 7×10^6 at 4 K, so sufficiently high Q values can probably be achieved in large aluminum antennas if a multimode matching network is used. A quantum limited antenna with $m_1 = 2000$ kg could detect a 1-msec pulse with $h = 2\times10^{-21}$ at a SNR of unity, and with six modes it would have a bandwidth of 300 Hz.

There is one important limitation to the analysis presented in this paper. It has been supposed that the mechanical-amplifier noise parameters are fixed, and then optimal values of the matching masses and springs have been computed. This program can run into difficulty if the design of the mechanical amplifier imposes constraints on the values of the last mass and spring that are in conflict with the optimal values. For superconducting variable inductance transducers, the most important constraint is that the last spring cannot be less than the magnetic spring that results from the stored supercurrent. For designs that are presently contemplated, it turns out that the magnetic spring is less than the last spring required by the maximally flat networks, so no difficulty arises. However, for mechanical amplifiers with very small values of R_n, the transducer design constraints may not allow the use of maximally flat networks. In particular, the last mass required by a

maximally flat design may become too small. This is the case for the very sensitive mechanical amplifier used by the Rome group, which uses an electrostatic transducer. Such mechanical amplifiers will require higher mechanical Q values than amplifiers that can use the maximally flat networks, but this may not be a prohibitive disadvantage, at least in the next generation. The optimal design problem for transducers with small R_n values is doubly constrained. One must find, for a given value of R_n, networks that are as broadband and flat as possible with both m_1 and the last mass specified. This is an open problem.

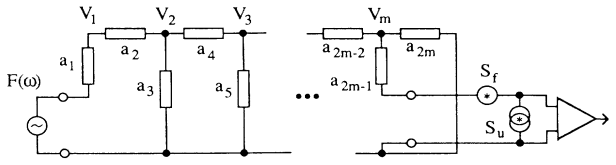

FIG. 11. Electrical analog circuit for a multimode antenna with m normal modes. The a_i with i even are series branch impedances, and the a_i with i odd are shunt branch admittances. The V_i represent node voltages.

ACKNOWLEDGMENTS

I would like to thank Robert Taber for many helpful discussions, and Thomas Stevenson, Peter Michelson, Katrina Lane, and William Fairbank for their comments. This work was supported by the National Science Foundation under Grant No. PHY85-05755.

APPENDIX A: EVALUATION OF THE SIGNAL-TO-NOISE RATIO OF MULTIMODE ANTENNAS

To evaluate the SNR of the multimode lumped element model (Fig. 4) it is necessary to compute the transfer admittance y_{21} and the output admittance y_{22} that appear in Eq. (7). An electrical analog for the multimode model is given in Fig. 11. As in Fig. 5, the classical analog is used, in which voltage is analogous to force, current to velocity, inductance to mass, and capacitance to inverse spring constant. The a_i with i even represent series branch impedances, and the a_i with i odd represent shunt branch admittances. Kuh and Pederson have shown how in this notation the determinant and cofactors of a ladder network may be written very compactly.[28] The even a_i are the impedances of the masses:

$$a_2 \equiv sm_1, \quad a_4 \equiv sm_2, \quad \ldots, \quad a_{2m} \equiv sm_m , \tag{A1}$$

where s is the complex frequency variable, $s \equiv \rho + j\omega$. The odd a_i are the admittances of the springs and the dissipative elements in the series

$$\begin{aligned} a_1 &\equiv \frac{1}{d_1 + \dfrac{k_1}{s}} = \frac{s}{\omega_1 m_1 (\omega_1 + s/Q_1)} , \\ a_2 &\equiv \frac{s}{\omega_2 m_2 (\omega_2 + s/Q_2)}, \quad \ldots , \\ a_{2m-1} &\equiv \frac{s}{\omega_m m_m (\omega_m + s/Q_m)} . \end{aligned} \tag{A2}$$

With respect to the node voltages V_i indicated in Fig. 11 the determinant of the node equations may be written as

$$\Delta = \begin{vmatrix} a_1 + \dfrac{1}{a_2} & -\dfrac{1}{a_2} & 0 & & & \\ -\dfrac{1}{a_2} & \dfrac{1}{a_2} + a_3 + \dfrac{1}{a_4} & -\dfrac{1}{a_4} & & & \\ 0 & -\dfrac{1}{a_4} & \ddots & \ddots & & \\ & & \ddots & & -\dfrac{1}{a_{2m-2}} & \\ & & & -\dfrac{1}{a_{2m-2}} & \dfrac{1}{a_{2m-2}} + a_{2m-1} + \dfrac{1}{a_{2m}} \end{vmatrix} . \tag{A3}$$

Kuh and Pederson show that this tridiagonal and symmetric determinant can be written in terms of the simple continuant K_j, which is defined by

$$\begin{aligned} &K_0 = 1, \quad K_1 = a_1, \quad K_2 = a_2 K_1 + K_0 , \\ &K_3 = a_3 K_2 + K_1, \quad \ldots , \quad K_j = a_j K_{j-1} + K_{j-2} . \end{aligned} \tag{A4}$$

Their expression for the determinant is

$$\Delta = \frac{K_{2m}}{a_2 a_4 \cdots a_{2m}} . \tag{A5}$$

The driving-point impedance Z_{mm} at the last node is given by

$$Z_{mm}=\frac{\Delta_{mm}}{\Delta}=a_{2m}\frac{K_{2m-2}}{K_{2m}}\ , \tag{A6}$$

where Δ_{mm} is the cofactor, and the open-circuit transfer impedance Z_{m1} from the first node to the last is given by

$$Z_{m1}=\frac{\Delta_{1m}}{\Delta}=\frac{a_{2m}}{K_{2m}}\ . \tag{A7}$$

Z_{mm} and Z_{m1} may be related to y_{22} and y_{21}:

$$y_{22}=a_{2m-1}(1-Z_{mm}a_{2m-1})$$

$$=a_{2m-1}\left[1-a_{2m}a_{2m-1}\frac{K_{2m-2}}{K_{2m}}\right]\ , \tag{A8a}$$

$$y_{21}=a_1a_{2m-1}Z_{m1}=\frac{a_1a_{2m-1}a_{2m}}{K_{2m}}\ . \tag{A8b}$$

These expressions, together with the definitions (A1), (A2), and (A4) and the SNR integral Eq. (7) (to which the correlation noise term may be added), provide a basis for a numerical solution to the SNR analysis problem for multimode antennas. A simple way to proceed is to fix the frequency, evaluate the complex numbers a_i, evaluate K_{2m-2} and K_{2m}, evaluate y_{22} and y_{21}, evaluate the integrand of Eq. (7), and then to repeat this process at many frequencies to find the integrand $\sigma(\omega)$, and finally to integrate numerically to find the SNR.

APPENDIX B: MAXIMALLY FLAT APPROXIMATION

By writing out the derivatives it can be shown that a function $F(\Omega^2)$ will have all derivatives up to and including the kth equal to zero at $\Omega=\pm1$ if and only if the function $F(x)$ has all derivatives with respect to x up to and including the kth equal to zero at $x=1$. To find the maximally flat magnitude function it is thus sufficient to find a function of the form

$$F(x)\propto\frac{x^3}{\sum_{i=0}^{2m}a_ix^i} \tag{B1}$$

with as many derivatives as possible equal to zero at $x=1$. Writing $F=N/D$ and setting the derivative at $x=1$ to zero, one finds that $ND^{(1)}=N^{(1)}D$ at $x=1$. (A superscript in parentheses indicates the number of derivatives taken.) Using this equation and setting the second derivative of F at $x=1$ to zero, one finds that $ND^{(2)}=N^{(2)}D$ at $x=1$. Continuing in this way, it can be shown that the relations

$$ND^{(1)}=N^{(1)}D,\quad ND^{(2)}=N^{(2)}D,\quad \ldots\ ,\quad ND^{(k)}=N^{(k)}D \tag{B2}$$

hold at $x=1$ if all of the derivatives of F up to and including the kth are zero at $x=1$.

If D is expressed as a power series about $x=1$,

$$D=\sum_{i=0}^{2m}b_i(x-1)^i\ , \tag{B3}$$

and if $N=x^3$, then Eqs. (B2) become

$$b_1=3b_0,\quad 2b_2=6b_0,\quad 6b_3=6b_0\ ,\quad b_4=0,\quad \ldots\ ,\quad b_k=0\ . \tag{B4}$$

Substituting these relations back into Eq. (B3) gives

$$D=\sum_{i=k+1}^{2m}b_i(x-1)^i+b_0x^3\ . \tag{B5}$$

The largest value that k can take is $k=2m-1$ because otherwise F reduces to a constant. Thus, the maximally flat function with all derivatives up to and including the $(2m-1)$th equal to zero at $x=1$ is

$$F(x)\propto\frac{x^3}{b_{2m}(1-x)^{2m}+b_0x^3}\ . \tag{B6}$$

Substituting $x=\Omega^2$ now gives Eq. (31) for $m=2,3,\ldots$, and a similar argument can be made for the $m=1$ case.

[1]K. S. Thorne, Rev. Mod. Phys. **52**, 285 (1980); L. Smarr, *Sources of Gravitational Radiation* (Cambridge University Press, Cambridge, England, 1979); J. A. Tyson and R. P. Giffard, Annu. Rev. Astron. Astrophys. **16**, 521 (1978).

[2]J. Weber, Phys. Rev. **117**, 306 (1960); Phys. Rev. Lett. **17**, 1228 (1966).

[3]*Proceedings of the IV Marcel Grossmann Meeting on General Relativitiy,* Rome, 1985, edited by R. Ruffini (North-Holland, Amsterdam, 1986).

[4]R. W. P. Drever, in *General Relativity and Gravitation,* Padua, 1983, edited by B. Bertotti, F. de Felice, and A. Pascolini (Reidel, Dordrecht, 1984).

[5]R. P. Giffard, Phys. Rev. D **14**, 2478 (1976).

[6]An exception is the Tokyo group, see M.-K. Fujimoto, in *Proceedings of the Second Marcel Grossmann Meeting on General Relativity,* Trieste, 1979, edited by R. Ruffini (North-Holland, Amsterdam, 1982).

[7]P. F. Michelson and R. C. Taber, Phys. Rev. D **29**, 2149 (1984).

[8]H. Rothe and W. Dahlke, Proc. IRE **44**, 811 (1956).

[9]L. A. Wainstein and V. D. Zubakov, *Extraction of Signals from Noise* (Prentice-Hall, Englewood Cliffs, NJ, 1962), Chap. 3.

[10]J. B. Johnson, Phys. Rev. **32**, 97 (1928); H. Nyquist, *ibid.* **32**, 110 (1928); J. L. Lawson and G. E. Uhlenbeck, *Threshold Signals* (McGraw-Hill, New York, 1950), Chap. 4.

[11]There are exceptional cases in which energy can be trapped in modes that are completely decoupled from the noise resistance. The center-of-mass motion of an isolated mechanical system is an example.

[12]S. P. Boughn *et al.*, Astrophys. J. Lett. **261**, L19 (1982), and references therein.

[13]J.-P. Richard, in *Proceedings of the Second Marcel Grossmann Meeting on General Relativity* (Ref. 6); Phys. Rev. Lett. **52**,

165 (1984).
[14]H. J. Paik, in Abstracts of the 11th International Conference on General Relativity and Gravitation, Stockholm, 1986 (unpublished).
[15]M. Karim, Phys. Rev. D **3**, 2031 (1984), and references therein; D. G. Blair, A. Giles, and M. Zeng, J. Phys. D **20**, 162 (1987).
[16]P. F. Michelson and R. C. Taber, J. Appl. Phys. **52**, 4313 (1981); J.-P. Richard, *ibid.* **60**, 3807 (1986); M. Bassan, Nuovo Cimento C **7**, 303 (1984).
[17]D. G. Blair, in *Gravitational Radiation, Collapsed Objects, and Exact Solutions,* proceedings of the Einstein Centenary Summer School, Perth, 1979, edited by C. Edwards (Springer, Berlin, 1980); K. Tsubono, M. Ohashi, and H. Hirakawa, Jpn. J. Appl. Phys. **25**, 622 (1986); P. Rapagnani, Nuovo Cimento C **5**, 385 (1982).
[18]H. J. Paik, J. Appl. Phys. **47**, 1168 (1976).
[19]J. E. Storer, *Passive Network Synthesis* (McGraw-Hill, New York, 1957), Chap. 22; E. A. Guillemin, in *Advances in Electronics,* edited by L. Marton (Academic, New York, 1951), Vol. III, pp. 261–303; W. Cauer, *Synthesis of Linear Communication Networks* (McGraw-Hill, New York, 1958).
[20]L. Weinberg, *Network Analysis and Synthesis* (McGraw-Hill, New York, 1962); H. Baher, *Synthesis of Electrical Networks* (Wiley, New York, 1984).
[21]Storer, *Passive Network Synthesis* (Ref. 19), Chap. 19.
[22]Weinberg, *Network Analysis and Synthesis* (Ref. 20), p. 83.
[23]Weinberg, *Network Analysis and Synthesis* (Ref. 20), Chap. 11.
[24]Storer, *Passive Network Synthesis* (Ref. 19), Chap. 7.
[25]Weinberg, *Network Analysis and Synthesis* (Ref. 20), Chap. 9; Baher, *Synthesis of Electrical Networks* (Ref. 20), Chap. 3; Cauer, *Synthesis of Linear Communication Networks* (Ref. 19), Chap. 5.
[26]Weinberg, *Network Analysis and Synthesis* (Ref. 20), Chap. 5.
[27]E. Amaldi *et al.*, in *Proceedings of the IV Marcel Grossmann Meeting on General Relativity* (Ref. 3).
[28]E. S. Kuh and D. O. Pederson, *Principles of Circuit Synthesis* (McGraw-Hill, New York, 1959), Appendix 1.